DOI: 10.1002/adma.201703357
Article type: Communication

Electrochemical Tantalum Oxide for Resistive Switching Memories

Andrea Zaffora, Deok-Yong Cho, Kug-Seung Lee, Francesco Di Quarto, Rainer Waser, Monica Santamaria, and Ilia Valov**

Advanced Materials 29 (43) (2017) 1703357

A. Zaffora, Prof. F. Di Quarto, Prof. M. Santamaria
Electrochemical Materials Science Laboratory, DICAM, Palermo University, Palermo 90128, Italy
E-mail: monica.santamaria@unipa.it

Dr. D.-Y. Cho
IPIT & Department of Physics, Chonbuk National University, Jeonju 54896, Korea

Dr. K.-S. Lee
Pohang Accelerator Laboratory, Pohang 37673, Korea

Prof. R. Waser, Dr. I. Valov
Institut für Werkstoffe der Elektrotechnik 2, RWTH Aachen University, 52074 Aachen, Germany
Peter Grünberg Institute, Forschungszentrum Jülich, 52425 Jülich, Germany
E-mail: i.valov@fz-juelich.de

Keywords: resistive switching, anodic thin films, ReRAMs, tantalum oxide, multilevel

Redox-based resistive switching memories (ReRAMs) are strongest candidates for the next generation nonvolatile memories fulfilling the criteria for fast, energy efficient and scalable green IT. These type of devices can also be used for selector elements, alternative logic circuits and computing, memristive and neuromorphic operations. ReRAMs are composed by metal/solid electrolyte/metal junctions in which the solid electrolyte is typically a metal oxide or multilayer oxides structures. Here we offer an effective and cheap electrochemical approach to fabricate Ta/Ta_2O_5-based devices by anodizing. This method allows to grow high quality and dense oxides thin film onto a metallic substrates with precise control over morphology and thickness. Electrochemical oxide based devices demonstrate superior properties i.e. - endurance of at least 10^6 pulse cycles and/or 10^3 *I-V* sweeps maintaining a good memory window with a low dispersion in R_{OFF} and R_{ON} values, nanosecond fast switching and data retention of at least 10^4 seconds. Multilevel programming capability is presented with both *I-V* sweeps and pulse measurements. Thus, it is shown that anodizing has a great prospective as a method for preparation of dense oxide films for resistive switching memories.

Redox-based resistive switching memories (ReRAMs) are strongest candidates for the next generation nonvolatile memories fulfilling the criteria for fast, energy efficient and scalable green IT.[1–6] These type of devices can also be used for selector elements,[7] alternative logic circuits and computing,[8–11] memristive and neuromorphic operations.[12–15] ReRAMs are composed by metal/solid electrolyte/metal junctions in which the solid electrolyte is often a metal oxide or multilayer oxides structures. In last decade ReRAMs have been intensively investigated to understand in details the switching kinetics and the microscopic ionic/electronic mechanisms in order to improve the retention and endurance and to optimize

device performance.[2] Most attractive are the filament type switching systems based on a change in electrolyte resistance due to the formation/dissolution of electronically conducting filaments that short circuit the metal electrodes leading the device from a high (HRS) to a low resistance state (LRS). Filament formation and dissolution are the consequence of electrode redox reactions at the metal/electrolyte interfaces and of the movement of the ions, generated by these reactions.[1] Depending on the materials used in the devices and processes leading to resistive switching, two types of bipolar ReRAM memories are distinguished: ECMs (Electrochemical Metallization Memories) and VCMs (Valence Change Memories). ECM cells are related to the oxidation of an active electrode (usually Cu or Ag), movement of cations into the electrolyte and consequent cations reduction at the inert electrode with the formation/dissolution of metallic filaments. In the case of VCM cells, resistive switching is described with the formation of an oxygen deficient filament for the SET process that can be re-oxidized leading to its partial dissolution (RESET). Oxygen anions movement is supposed to be responsible for the resistive switching in these cells although recently also cations movement was demonstrated by several authors.[16–19]

Solid oxide electrolytes for ReRAMs, are usually prepared by means of atomic layer deposition, chemical vapor deposition, pulsed laser deposition or RF sputtering.[2,5,20] Despite these techniques are largely used for producing high quality thin films for nanoelectronics, these methods require high/ultrahigh vacuum conditions and in many cases the high energy particles penetrate into the underlying matrix inducing interface mixing of materials. An alternative way to produce high quality metal oxides is the electrochemical anodizing. This is a non-vacuum, low-temperature, low-cost process that allows to grow oxide films on the surface of valve metals (such as Ta, Ti, Hf, Zr, Al, Nb etc.) and valve metals alloys. Anodizing is typically carried out in liquid electrolytes where the metal substrate is oxidized by applying an anodic polarization. The metal cations M^{z+} react with oxygen anions O^{2-} provided by the electrolyte, thus producing the anodic film according the reaction:

$$M + xH_2O \rightarrow MO_x + xH_2 \quad (1)$$

The oxide grows by field-assisted transport ($E \sim 10^6 - 10^7$ V cm^{-1}) trigged by metal cations and oxygen anions with film expanding at metal/oxide or oxide/electrolyte interface depending on transport (transference) number of the particular ions. As shown in **Figure 1a** for the case of anodic formation of Ta_2O_5, both ionic species can contribute to the transport/growth with a cation transport number for Ta^{5+} reported to vary between 0.14 and 0.32 depending on anodizing conditions.[21,22] Most important, anodizing allows to grow oxides with well-defined characteristics such as thickness, composition, structure and morphology by easily controlling operating parameters such as formation potential, growth rate, electrolyte and metal substrate compositions.[23–29] In the case of anodizing of metallic alloys, resulting oxide will be a mixed oxide in which the atomic ratio between partner metals can be different with respect to the underlying alloys depending on transport numbers of involved cations. To date, there are several papers in which porous anodic aluminum oxide is used as a matrix for the fabrication of ReRAMs [30–33] or anodic nanostructured oxides are used as solid electrolytes,[34–38] but only few papers discuss on ReRAMs devices with barrier-type anodic oxides however not showing some particular promises.[39–42]

Here we demonstrate Ta/Ta_2O_5/Pt system with electrochemically grown Ta_2O_5 showing superior performance. The devices based on electrochemical tantalum oxide show ultra-fast switching times i.e. SET time of 20 ns (at V_{SET} = 1.25 V) and RESET time of 165 ns (at V_{RESET} = - 1.9 V), high endurance of over 10^6 cycles and retention over 10^4 s. These values are only limited by the equipment feasibility. The cells can reliably provide multilevel switching, with finely defined stable resistance values and negligible resistance dispersion. Firstly we have investigated the electrochemical reactions in the system preceding the resistive switching. Cyclic voltammetry measurements (CV) shown in Figure 1b reveal at

least three different processes. In the first cycle only one redox peak is well-resolved, related to an oxidation reaction, recorded at positive voltage of V_1 = 2.1 V. This peak merges and is further not clearly distinguishable during subsequent cycles. Within the sweep in the negative voltage range we observe reduction processes (or process) that appear within the range of +1 V and –1 V. However, no distinguished peak(s) can be resolved and for this reason we mark this region in Figure 1b by V_{red}, without indexing. During the reduction process(es) obviously new species are formed because on the second positive sweep scan we detect a new oxidation peak at V_2 = 1.3 V. It merges with V_1 and forms a plateau in the range 1.3 V to 2.5 V. Increasing the voltage over + 3 V leads to a formation of filament i.e. resistive switching. In order to more clearly distinguish the individual redox peaks, we used a sweep rate of 900 mV s^{-1}, higher with respect to that used in literature for same measurements with same materials.[19] Several electrode reactions are possible, including the Ta/Ta^{x+} and O/O^{2-} half-cell reactions but also those related to moisture:[19]

$$Ta \rightleftharpoons Ta^{x+} + xe^- \quad (2)$$

$$2O^{2-} \rightleftharpoons O_2 + 4e^- \quad (3)$$

$$2OH^- \rightleftharpoons 1/2\, O_2 + H_2O + 2e^- \quad (4)$$

$$2OH^- + H_2 \rightleftharpoons 2H_2O + 2e^- \quad (5)$$

$$2H_2O \rightleftharpoons O_2 + 4H^+ + 4e^- \quad (6)$$

CVs are classically recorded in a three electrodes configuration to exactly identify redox potential of any peaks with respect to the reference electrode potential. In this case, a reference electrode is not available and it is difficult to identify the exact electrochemical reaction related to every redox peak. For positive voltages oxidation of Ta is the most probable from a thermodynamic point of view with a possible further chemical reaction of the metal cation with O^{2-} and/or OH^- to form Ta oxide or hydroxide.[19] Nevertheless, since all the

measurements have been performed in ambient atmosphere, the influence of water molecules bonded on TaO_x matrix cannot be excluded, with particular reference to oxygen reduction reaction to form OH^- ions and water decomposition to form molecular oxygen.[19,43] It is also important to mention that the anodic Ta oxide we used for the experiments is much denser compared to same oxides (and composition) prepared by physical deposition techniques, that resulted in nanoporous structures which can easily host water molecules.[44] For this reason we assume that the redox peaks are related to reactions (2 and 3) rather than to reactions (4-6).

In **Figure 2a** we show a selected number of *I-V* sweeps of 10^3 consecutive cycles on a single device. The device shows bipolar, eight-wise switching with low switching voltages, V_{SET} ranging between 0.45 and 0.65 V and V_{RESET} ranging between -0.55 and -0.65 V. The low voltage variability proves that the memory device exhibits high uniformity in SET and RESET processes with narrow distribution. As shown in Figure 2b, R_{OFF} and R_{ON} are almost constant with the number of cycles, maintaining a R_{OFF}/R_{ON} ratio > 10, standard requirement to use these devices for memory applications.[45] By variation of the current compliance we were able to demonstrate multilevel switching with at least 9 adjustable resistance levels as shown in Figure 2c and 2d. By increasing I_C, R_{ON} decreases from 3870 (I_C = 100 μA) to 85 Ω (I_C = 10 mA) (see Figure 2e). The different resistance values are determined by changes in the thickness of the filament and/or by the change of the composition (oxidation state) of both filament and disc. These resistances were shown to be stable and do not vary within the time of the observation (Figure 2c and 2d).

Further measurements on the device performance and stability were performed using rectangular voltage pulses. The samples could be switched to the LRS as fast as 20 ns at 1.25 V. Also very short RESET times were achieved of 165 ns at -1.9 V.

The endurance of the devices was tested at SET pulses of 0.8 V (t_{SET} ~ 75 ns) and RESET pulses of -1.2 V (t_{RESET} < 200 ns). The READ operation was performed at 200 mV with 2.5 ms pulse length. The sequence of the cycles were: READ, SET, READ, RESET. In these

experiments we demonstrated endurance better than 10^6 cycles without degeneration of the ON and OFF states (see **Figure 3a**).

The retention of the LRS has also been confirmed to be at least 10^4 s without any sign of degeneration as shown in Figure 3b. It has been performed at 20 mV every 20 s with a 100 ms READ pulse. RESET process was successfully performed after every retention test without any change in the value for the V_{RESET}. These performances are comparable to that obtained by devices prepared through sputtering deposition process or even better.[46] The excellent stability of the current during retention tests indicate that much longer retention times and endurance can be easily reached by the devices.

The reason for this superior performance of the electrochemical oxide film is originating in the specifics of the physical properties of the film, predetermined by the method of preparation. XRR measurements have shown that the film density of 8.5 g cm^{-3} is much higher compared to Ta_2O_5 films prepared by RF sputtering, reactive sputtering or e-beam evaporation techniques that vary between 6.2 g cm^{-3} and 7.6 g cm^{-3}.[44]

Density is closely related to the transport properties of thin films. In general, lower density (higher porosity) is lowering the ion diffusion as the path of an ion to pass same effective distance becomes longer and/or related to overcoming additional energetic barriers. Density is especially important for ReRAMs regarding effects of moisture.[44] Lower density supports higher uptake, and higher density – lower uptake of moisture. The amount of absorbed moisture significantly changes the ReRAM performance.[19,47] Moisture is reported to be essential component in ReRAMs, at least for the forming step.[43,44] No unequivocal answer is given on the question whether moisture is also so essential for the following SET/RESET operations. On the other hand, since Ta is less noble than water,[48] moisture can promote Ta oxidation (according to equation 1) i.e. should decrease the stability.[49] The oxidation of Ta is additionally enhanced by applying a positive voltage to the Ta electrode during cycling. Thus,

density appears a factor in ReRAMs influencing the transport and stability directly (diffusion), and indirectly (uptake of moisture).

In the ideal case the Ta_2O_5 should contain some moisture (to enable forming and possibly support faster switching) but not too much as it will affect the stability. From measurements carried out in vacuum conditions, the electrochemical Ta_2O_5 films follow this trend thus contain enough moisture to allow forming but also less enough to avoid metal oxidation and thus, support higher stability for good retention and fine dispersed multilevel switching.

Thus, we show that electrochemical anodizing is a reliable and prospective method for fabrication of high quality thin oxide films for resistive switching memories.

In conclusion, we have shown superior performance of a $Ta/Ta_2O_5/Pt$ system based on electrochemically grown Ta oxide. This method is suggested as an alternative way to prepare solid electrolytes for ReRAM devices. *I-V* cycling and pulse endurances have been demonstrated for at least 10^3 and 10^6 cycles, respectively with high stability and low dispersion of SET and RESET voltages and excellent data retention. Stable resistance window and capability for at least 9 distinguished multilevels have been achieved. Switching times in the low nanosecond range were demonstrated.

Electrochemical anodizing is a reliable alternative way to prepare well defined and cost-effective solid electrolytes for ReRAM devices.

Experimental Section

Electrochemical oxide growth and devices fabrication: Ta was sputtering-deposited on glass substrate with a thickness of ~ 280 nm. Ta_2O_5 anodic growth was carried out at room temperature in a three electrodes cell configuration with Ta as working electrode, platinum net with high surface area was the counter electrode and a silver/silver chloride/sat. KCl (SSC) reference electrode (0 V vs. Ag/AgCl = 0.197 V vs. SHE). The anodizing electrolyte was a borate buffer (0.42 mol l^{-1} H_3BO_3, 0.08 mol l^{-1} $Na_2B_4O_7$) (pH = 8), in which Ta_2O_5 is

thermodynamically stable according to Pourbaix's diagram (relative to Ta-H_2O at room temperature).[48] Two different oxide thicknesses were obtained by controlling formation potential U_F: 20 nm (U_F = 10 V vs. SSC) and 40 nm (U_F = 20 V vs. SSC). The anodic oxide films are amorphous,[24] smooth[50] and uniform in thickness and composition.[24] Layer density was evaluated by X-Ray Reflectivity (XRR) measurements (PANalytical XPert Pro with copper anode (Cu Kα radiation, λ = 0.15405 nm) over the angle range 0.3 – 2.5°). The estimated density value of 8.5 g $cm^{-3}$is higher with respect to the densities of Ta_2O_5 films prepared through EB deposition or sputtering.[44] 50 nm Pt top electrode was sputtered on the anodic films and then structured by photolithography and lift-off processes. The electrode pad sizes were between 25×25 and 100×100 μm^2.

Electrical characterization: CV measurements were performed with a Keithley 6430 Sub-FemtoAmp Remote SourceMeter in ambient atmosphere. I-V sweeps, retention and endurance tests were carried out by using a Keithley 2636 A System SourceMeter. Fast pulse measurements were performed with a Keithley 4200-SCS Semiconductor Characterization System. In all the measurements, voltage was applied to the Ta bottom electrode with Pt top electrode grounded.

Acknowledgements
The authors (A.Z., F.D.Q. and M.S.) acknowledge Professor H. Habazaki (Graduate School of Engineering, Hokkaido University, Japan) for providing sputtering-deposited Ta. The authors acknowledge Daliborka Erdoglija for the fabrication of Pt top electrodes and Thomas Pössinger for the help with graphics (IWE 2, RWTH Aachen University, Germany).

Received: ((will be filled in by the editorial staff))
Revised: ((will be filled in by the editorial staff))
Published online: ((will be filled in by the editorial staff))

References

[1] I. Valov, *ChemElectroChem* **2014**, *1*, 26.

[2] D. Ielmini, R. Waser, Eds. , *Resistive Switching: From Fundamentals of Nanoionic*

Redox Processes to Memristive Device Applications, Wiley-VCH Verlag GmbH & Co. KGaA, Weinheim, Germany, **2016**.

[3] T. Hasegawa, K. Terabe, T. Tsuruoka, M. Aono, *Adv. Mater.* **2012**, *24*, 252.

[4] R. Waser, M. Aono, *Nat. Mater.* **2007**, *6*, 833.

[5] M.-J. Lee, C. B. Lee, D. Lee, S. R. Lee, M. Chang, J. H. Hur, Y.-B. Kim, C.-J. Kim, D. H. Seo, S. Seo, U.-I. Chung, I.-K. Yoo, K. Kim, *Nat. Mater.* **2011**, *10*, 625.

[6] A. C. Torrezan, J. P. Strachan, G. Medeiros-Ribeiro, R. S. Williams, *Nanotechnology* **2011**, *22*, 485203.

[7] R. Midya, Z. Wang, J. Zhang, S. E. Savel'ev, C. Li, M. Rao, M. H. Jang, S. Joshi, H. Jiang, P. Lin, K. Norris, N. Ge, Q. Wu, M. Barnell, Z. Li, H. L. Xin, R. S. Williams, Q. Xia, J. J. Yang, *Adv. Mater.* **2017**, *29*, 1604457.

[8] J. J. Yang, D. B. Strukov, D. R. Stewart, *Nat. Nanotechnol.* **2013**, *8*, 13.

[9] E. Linn, R. Rosezin, S. Tappertzhofen, U. Böttger, R. Waser, *Nanotechnology* **2012**, *23*, 305205.

[10] J. Borghetti, G. S. Snider, P. J. Kuekes, J. J. Yang, D. R. Stewart, R. S. Williams, *Nature* **2010**, *464*, 873.

[11] Y. V. Pershin, M. Di Ventra, *IEEE Trans. Circuits Syst. I Regul. Pap.* **2010**, *57*, 1857.

[12] T. Ohno, T. Hasegawa, T. Tsuruoka, K. Terabe, J. K. Gimzewski, M. Aono, *Nat. Mater.* **2011**, *10*, 591.

[13] Z. Wang, S. Joshi, S. E. Savel'ev, H. Jiang, R. Midya, P. Lin, M. Hu, N. Ge, J. P. Strachan, Z. Li, Q. Wu, M. Barnell, G.-L. Li, H. L. Xin, R. S. Williams, Q. Xia, J. J. Yang, *Nat. Mater.* **2017**, *16*, 101.

[14] C. Du, W. Ma, T. Chang, P. Sheridan, W. D. Lu, *Adv. Funct. Mater.* **2015**, *25*, 4290.

[15] M. Prezioso, F. Merrikh-Bayat, B. D. Hoskins, G. C. Adam, K. K. Likharev, D. B. Strukov, *Nature* **2015**, *521*, 61.

[16] A. Wedig, M. Luebben, D.-Y. Cho, M. Moors, K. Skaja, V. Rana, T. Hasegawa, K. K.

Adepalli, B. Yildiz, R. Waser, I. Valov, *Nat. Nanotechnol.* **2016**, *11*, 67.

[17] S. Privitera, G. Bersuker, B. Butcher, A. Kalantarian, S. Lombardo, C. Bongiorno, R. Geer, D. C. Gilmer, P. D. Kirsch, *Microelectron. Eng.* **2013**, *109*, 75.

[18] D. Carta, I. Salaoru, A. Khiat, A. Regoutz, C. Mitterbauer, N. M. Harrison, T. Prodromakis, *ACS Appl. Mater. Interfaces* **2016**, *8*, 19605.

[19] M. Lübben, P. Karakolis, V. Ioannou-Sougleridis, P. Normand, P. Dimitrakis, I. Valov, *Adv. Mater.* **2015**, *27*, 6202.

[20] N. Aslam, V. Longo, C. Rodenbücher, F. Roozeboom, W. M. M. Kessels, K. Szot, R. Waser, S. Hoffmann-Eifert, *J. Appl. Phys.* **2014**, *116*, 64503.

[21] J. P. S. Pringle, *J. Electrochem. Soc.* **1973**, *120*, 398.

[22] Q. Lu, P. Skeldon, G. E. Thompson, D. Masheder, H. Habazaki, K. Shimizu, *Corros. Sci.* **2004**, *46*, 2817.

[23] K. Shimizu, K. Kobayashi, G. E. Thompson, P. Skeldon, G. C. Wood, *Philos. Mag. Part B* **1996**, *73*, 461.

[24] H. Habazaki, K. Shimizu, P. Skeldon, G. E. Thompson, G. C. Wood, *Proc. R. Soc. A Math. Phys. Eng. Sci.* **1997**, *453*, 1593.

[25] P. Roy, S. Berger, P. Schmuki, *Angew. Chemie Int. Ed.* **2011**, *50*, 2904.

[26] F. Di Franco, M. Santamaria, F. Di Quarto, E. Tsuji, H. Habazaki, *Electrochim. Acta* **2012**, *59*, 382.

[27] W. Lee, S.-J. Park, *Chem. Rev.* **2014**, *114*, 7487.

[28] A. Zaffora, F. Di Franco, M. Santamaria, H. Habazaki, F. Di Quarto, *Electrochim. Acta* **2015**, *180*, 666.

[29] J. P. Kollender, A. I. Mardare, A. W. Hassel, *J. Electrochem. Soc.* **2017**, *164*, C598.

[30] U.-B. Han, J.-S. Lee, *Sci. Rep.* **2016**, *6*, 25537.

[31] A. Al-Haddad, C. Wang, H. Qi, F. Grote, L. Wen, J. Bernhard, R. Vellacheri, S. Tarish, G. Nabi, U. Kaiser, Y. Lei, *ACS Appl. Mater. Interfaces* **2016**, *8*, 23348.

[32] L.-Q. Qi, D.-Y. Pan, J.-Q. Li, L.-H. Liu, H.-Y. Sun, *Nanotechnology* **2017**, *28*, 115702.

[33] Y. Morishita, T. Hosono, H. Ogawa, *Solid. State. Electron.* **2017**, *131*, 30.

[34] N. Liu, K. Lee, P. Schmuki, *Angew. Chemie Int. Ed.* **2013**, *52*, 12381.

[35] S. Otsuka, T. Shimizu, S. Shingubara, K. Makihara, S. Miyazaki, A. Yamasaki, Y. Tanimoto, K. Takase, *AIP Adv.* **2014**, *4*, 87110.

[36] M. Bendova, J. Hubalek, A. Mozalev, *Adv. Mater. Interfaces* **2016**, *3*, 1600512.

[37] Y. Ji, Y. Yang, S.-K. Lee, G. Ruan, T.-W. Kim, H. Fei, S.-H. Lee, D.-Y. Kim, J. Yoon, J. M. Tour, *ACS Nano* **2016**, *10*, 7598.

[38] M. Marik, A. Mozalev, J. Hubalek, M. Bendova, *J. Phys. Conf. Ser.* **2017**, *829*, 12001.

[39] T. V. Kundozerova, A. M. Grishin, G. B. Stefanovich, A. A. Velichko, *IEEE Trans. Electron Devices* **2012**, *59*, 1144.

[40] T. V. Kundozerova, G. B. Stefanovich, A. M. Grishin, *Phys. Status Solidi* **2012**, *9*, 1699.

[41] W. Zhu, T. P. Chen, Y. Liu, S. Fung, *J. Appl. Phys.* **2012**, *112*, 63706.

[42] X. Yin, K. Tian, Z. Tan, R. Yang, X. Guo, *J. Electrochem. Soc.* **2015**, *162*, 271.

[43] T. Tsuruoka, K. Terabe, T. Hasegawa, I. Valov, R. Waser, M. Aono, *Adv. Funct. Mater.* **2012**, *22*, 70.

[44] T. Tsuruoka, I. Valov, S. Tappertzhofen, J. van den Hurk, T. Hasegawa, R. Waser, M. Aono, *Adv. Funct. Mater.* **2015**, *25*, 6374.

[45] D. J. Wouters, R. Waser, M. Wuttig, *Proc. IEEE* **2015**, *103*, 1274.

[46] A. Prakash, D. Jana, S. Maikap, *Nanoscale Res. Lett.* **2013**, *8*, 418.

[47] M. Lübben, S. Menzel, S. G. Park, M. Yang, R. Waser, I. Valov, *Nanotechnology* **2017**, *28*, 135205.

[48] M. Pourbaix, *Atlas of Electrochemical Equilibria in Aqueous Solutions*, Pergamon Press, Oxford, UK, **1966**.

[49] D.-Y. Cho, M. Luebben, S. Wiefels, K.-S. Lee, I. Valov, *ACS Appl. Mater. Interfaces*

2017, *9*, 19287.

[50] A. Zaffora, M. Santamaria, F. Di Franco, H. Habazaki, F. Di Quarto, *Phys. Chem. Chem. Phys.* **2016**, *18*, 351.

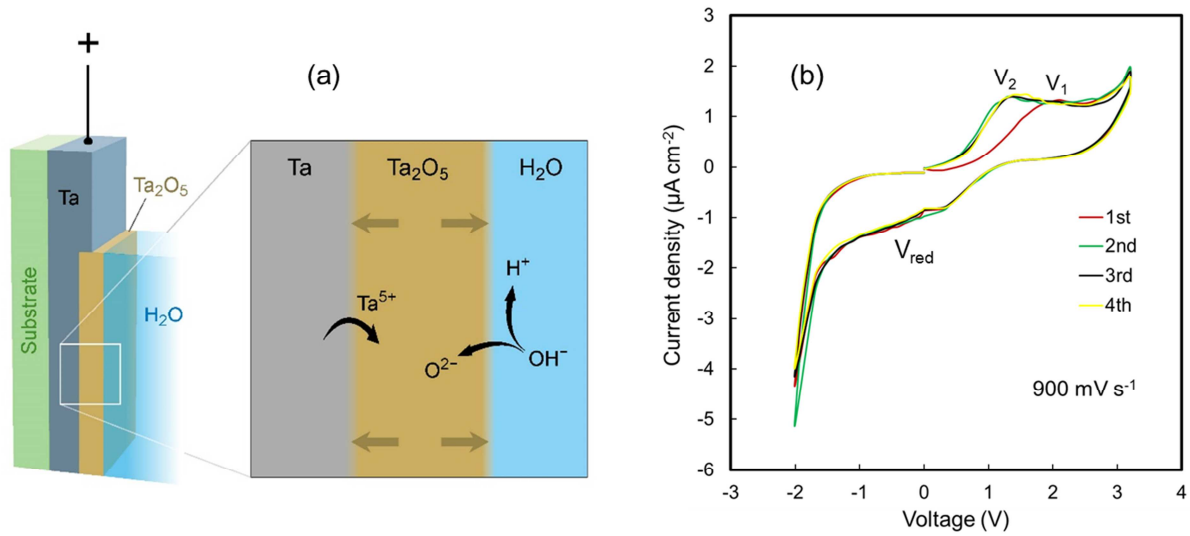

Figure 1. (a) Schematic electrochemical growth of anodic Ta_2O_5 layer. (b) Cyclic voltammogram of Ta/20 V Ta_2O_5/Pt cell recorded with a sweep rate of 900 mV s^{-1}. The measurements were performed in a proper voltage range (between -2 V and 3.2 V) in order to avoid the first SET process in the device.

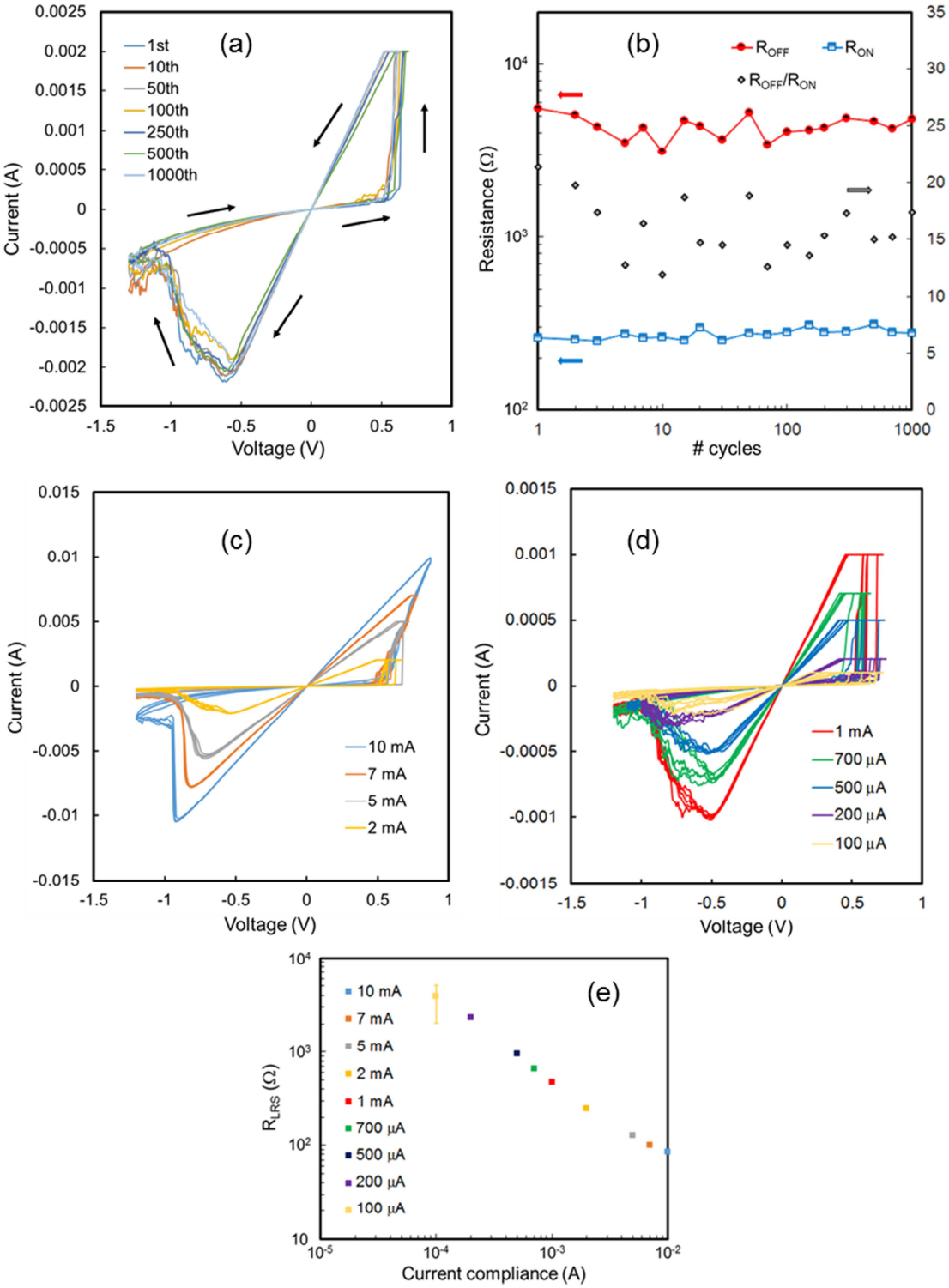

Figure 2. (a) 10^3 *I-V* cycles related to Ta/10 V Ta_2O_5/Pt cell and (b) resistance window during cycling the device. A current compliance of 2 mA was applied during this measurement. Resistances were calculated by Ohm's law at 0.1 V as read voltage for both HRS and LRS that vary between 6350 and 3100 Ω and between 250 and 320 Ω respectively. (c),(d) *I-V* sweeps recorded with different applied current compliances (between 10 mA and 100 µA). (e) LRS resistance vs. current compliance related to *I-V* sweeps shown in (c) and (d).

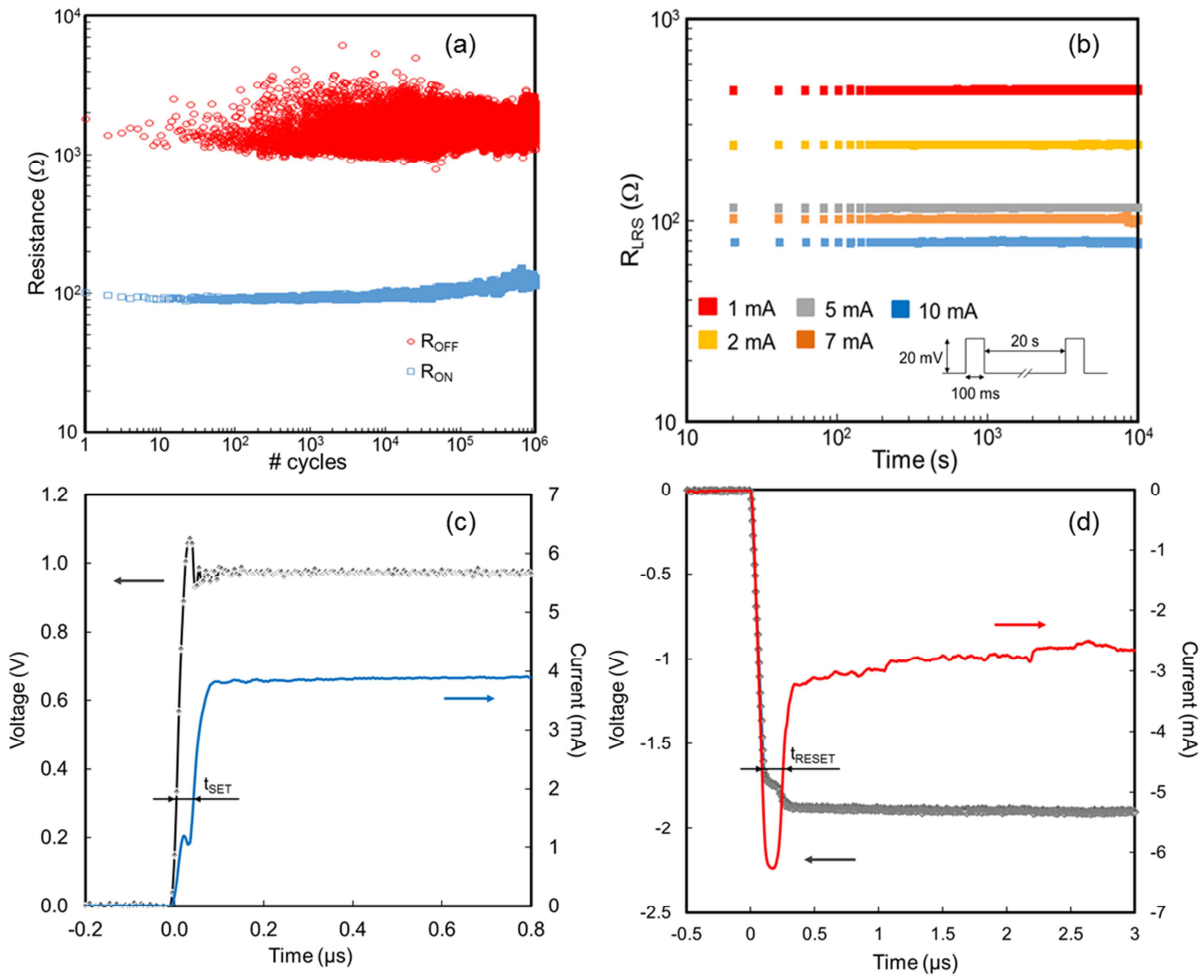

Figure 3. (a) Endurance test was performed by applying 2.5 ms pulses. Switching was carried out with V_{SET} = 0.8 V and V_{RESET} = -1.2 V and 0.2 V as read voltage. (b) Retention test for 5 different current compliances applied during the SET cycle preceding the test. A 20 mV pulse was applied every 20 s as shown in the inset. (c) SET pulse at 0.98 V and (d) RESET pulse at -1.9 V: switching time was evaluated as the time between the voltage rise and the half height of current rise after the peak related to the charging current of the cell capacitance.